Petroleum Science 21 (2024) 2614–2624

Contents lists available at ScienceDirect

Petroleum Science

journal homepage: www.keaipublishing.com/en/journals/petroleum-science

Original Paper

A unified fractional flow framework for predicting the liquid holdup in two-phase pipe flows

Fuqiao Bai , Yingda Lu *, Mukul M. Sharma

Hildebrand Department of Petroleum and Geosystems Engineering, The University of Texas at Austin, 200 E. Dean Keaton, Austin, TX, 78712, USA

ARTICLE INFO

Article history:
Received 12 February 2024
Received in revised form
30 April 2024
Accepted 7 May 2024
Available online 8 May 2024

Handling Editor: Dao-Yi Zhu
Edited by Yan-Hua Sun

Keywords:
Pipe fractional flow
Liquid holdup
Multiphase pipe flow
Gas void fraction

ABSTRACT

Two-phase pipe flow occurs frequently in oil & gas industry, nuclear power plants, and CCUS. Reliable calculations of gas void fraction (or liquid holdup) play a central role in two-phase pipe flow models. In this paper we apply the fractional flow theory to multiphase flow in pipes and present a unified modeling framework for predicting the fluid phase volume fractions over a broad range of pipe flow conditions. Compared to existing methods and correlations, this new framework provides a simple, approximate, and efficient way to estimate the phase volume fraction in two-phase pipe flow without invoking flow patterns. Notably, existing correlations for estimating phase volume fraction can be transformed and expressed under this modeling framework. Different fractional flow models are applicable to different flow conditions, and they demonstrate good agreement against experimental data within 5% errors when compared with an experimental database comprising of 2754 data groups from 14 literature sources, covering various pipe geometries, flow patterns, fluid properties and flow inclinations. The gas void fraction predicted by the framework developed in this work can be used as inputs to reliably model the hydraulic and thermal behaviors of two-phase pipe flows.

1. Introduction

Two-phase flow refers to the simultaneous flow of two distinct phases of matter (i.e., liquid–liquid, solid–liquid, solid–gas, gas–liquid, etc.), and is widely encountered in various industries, including refrigeration and air conditioning systems, nuclear power plants, microfluidic devices, and oil & gas production (Cioncolini and Thome, 2012; Li and Chen, 2023). In particular, two-phase pipe flows occur widely in the petroleum industry during the long-distance transportation of oil, gas, water, and CO_2 (Bai et al., 2023; Sun et al., 2022; Sunday et al., 2023; Teixeira et al., 2015). Accurate monitoring and control of the pressure, temperature, flow rate, and phase distribution of the flow are crucial for efficient hydrocarbon production (Gao et al., 2021; Jia et al., 2022; Sun et al. 2021a, 2021b). Some types of two-phase flows can induce cavitation, erosion, and slugging, causing potential damage to hardware and infrastructure, and must be carefully managed. All these operations need to be guided by reliable multiphase flow models.

One of the most significant unknown variables in two-phase pipe flow models is the void fraction (S_g) or its counterpart, the liquid holdup ($1 - S_g$), which is the volume fraction of the pipe occupied by the liquid phase at any given pipe cross-section. Once the phase volume fraction is obtained, some of the complex two-phase fluid flow problems can be treated in a manner that is analogous to single-phase fluid flow problems (Woldesemayat and Ghajar, 2007).

Numerous empirical void fraction models have been developed and these correlations can be broadly classified as: homogenous models, slip ratio models, K-factor models, drift flux models, and empirical models (Nagoo, 2014, 2019; Vijayan et al., 2000; Yu et al., 2023), with each category of model having its own intrinsic application conditions and limitations. For instance, the homogenous model (Woldesemayat, 2006) assumes a well dispersed flow distribution, which is not applicable in non-homogeneous flow systems. The slip ratio model is an empirical correlation that correlates the phase slip ratio, which is expressed as the ratio of liquid phase superficial velocity to gas phase superficial velocity, with the flow conditions. Lockhart and Martinelli (1949), Baroczy (1966), Fauske (1961), Spedding and Chen (1984), Zivi (1964) all present some well-known examples of slip ratio models. Slip-ratio models usually work well only in low-void-fraction flow systems such as

* Corresponding author.
E-mail address: yingdalu@austin.utexas.edu (Y. Lu).

https://doi.org/10.1016/j.petsci.2024.05.004

for bubble and annular flow. In the K-factor model, the void fraction is calculated by multiplying the homogenous void fraction by an empirical factor of K. Some widely used K-factor models are Armand (1946), Massena (1960), Hughmark (1962), and Czop et al. (1994) models. These simple correlations between void fraction and Reynolds number are invalid for many types of two-phase systems with significant pressure drops. The drift flux models are the most commonly used void fraction correlations in the literature and build on two empirical correlations of void fraction and drift velocity (Márquez-Torres et al., 2020). By coupling these two correlations, the phase volume distribution can be obtained. There are many drift flux models commonly used in two-phase flow, such as those developed by Nicklin (1962), Jowitt et al. (1984), Woldesemayat and Ghajar (2007), Choi et al. (2012), Bhagwat and Ghajar (2014), and Lou et al. (2023). Drift flux models usually have high computational cost and require the estimation of multiple variables including drift velocity and slip velocity. Finally, general empirical void fraction models, such as those developed by Zuber and Findlay (1965), Minami and Brill (1987), Abdul-Majeed (1996), Lockhart and Martinelli (1949), Baroczy (1966), and Fauske (1961), were derived from the experiments conducted under specified conditions, and can only be applied to one particular flow pattern (i.e., bubble, slug, and annular flow) and flow direction (i.e., either upward or downward flow).

The limitations of existing void fraction prediction methods necessitate a more robust approach. This study addresses this gap by introducing a simple and reliable modeling framework for determining the phase volume fractions over a wide range of two-phase flow conditions. Our model builds upon the pipe fractional flow theory presented in Nagoo and Sharma's work. In this paper, the model is tested and verified against an extensive experimental database and demonstrated high levels of reliability and applicability in all flow patterns.

2. Pipe fractional flow theory

2.1. Modeling framework

In a two-phase flow system, the fractional flow of phase i (f_i), is defined as the ratio of phase i volumetric flow rate (Q_i) to the sum of the phase volumetric flow rates. For two-phase flow,

$$f_i = \frac{Q_i}{Q_i + Q_j} \tag{1}$$

Dividing both the numerator and denominator of Eq. (1) by pipe cross-sectional area and using the fact that in multiphase pipe flow theory, superficial velocity (u) is defined as volumetric flow rate divided by pipe cross-sectional area, f_i can also be expressed as

$$f_i = \frac{u_i}{u_i + u_j} \tag{2}$$

where subscripts i, j denote a specified phase (e.g., gas, water, and oil); $u_i,\ u_j$ are the superficial velocities for phases i and j, m/s.

The superficial velocity (u) is expressed as the product of the actual fluid phase velocity (v) and phase volume fraction (S):

$$u_i = v_i S_i \tag{3}$$

Inserting Eq. (3) into Eq. (2), f_i can be obtained as

$$f_i = \frac{v_i S_i}{v_i S_i + v_j (1 - S_i)} \tag{4}$$

where v_i, v_j are the actual velocities for phases i and j, m/s; S_i represents the volume fraction of phase i; $1 - S_i$ is then the volume fraction of phase j. Note that $S_i + S_j = 1$ in a two-phase flow system.

We define a slip ratio R in our model, as the ratio of the actual velocities of the two fluid phases:

$$R_{i,j} = \frac{v_i}{v_j} \tag{5}$$

Inserting Eq. (5) into Eq. (4), the expression for the fractional flow can be rearranged and simplified as

$$f_i = \frac{R_{i,j}}{R_{i,j} + \dfrac{1 - S_i}{S_i}} \tag{6}$$

or,

$$S_i = \frac{1}{1 + \dfrac{1 - f_i}{f_i} R_{i,j}} \tag{7}$$

For instance, for a gas–liquid flow system, Eqs. (6) and (7) are expressed as

$$f_g = \frac{R_{g,l}}{R_{g,l} + \dfrac{1 - S_g}{S_g}} \tag{8}$$

or,

$$S_g = \frac{1}{1 + \dfrac{1 - f_g}{f_g} R_{g,l}} \tag{9}$$

where S_g is the gas void fraction; $R_{g,l}$ is the slip ratio of gas phase to liquid phase; f_g is the gas fractional flow.

Eqs. (6) and (7) indicate that the fractional flow (f_i) is strongly dependent on the phase volume fraction (S_i) and slip ratios ($R_{i,j}$). As an illustration, Fig. 1 plots the variations of fractional flow (f_i) with phase volume fraction (S_i) for different slip ratios ($R_{i,j}$). These fractional flow paths are either straight lines or curves depending on the values of the slip ratio.

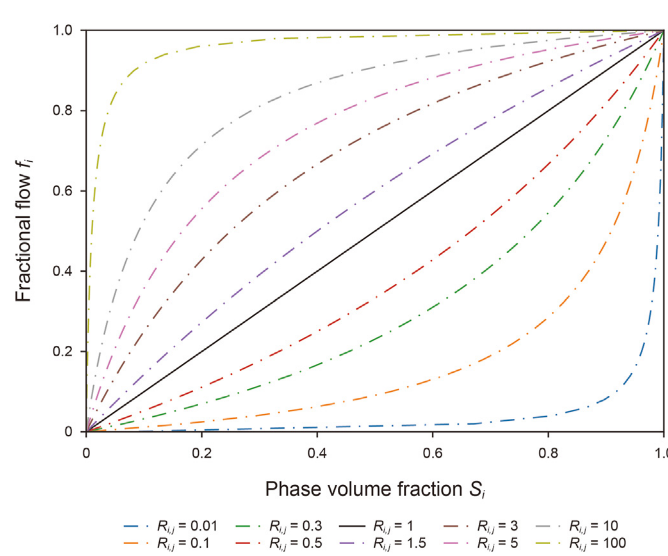

Fig. 1. General fractional flow path as a function of phase volume fraction (S_i) and slip ratios ($R_{i,j}$).

Therefore, a fractional flow curve defines the relationship between the phase fractional flow (f_i) and its phase volume fraction (S_i):

$$f_i = g(S_i, R_{i,j}) \tag{10}$$

However, this relationship is not unique and depends on a range of flow conditions. Further simplifications and assumptions regarding $R_{i,j}$ need to be made. Different assumptions for $R_{i,j}$ in Eq. (6) lead to different models that fit certain data sets. In this work, three simplified models will be presented in detail given their robustness in most two-phase fluid flow scenarios.

2.2. No-slip model

If no slippage occurs between different phases, $R_{i,j}$ will be obtained as

$$R_{i,j} = 1 \tag{11}$$

Substituting Eq. (11) into Eq. (6) yields

$$f_i = S_i \tag{12}$$

Eq. (12) is referred as the no-slip model. The fractional flow path for the no-slip model is presented in Fig. 2, and it is evident that this path is a straight line for all phase volumes. Fig. 2 also displays different flow patterns based on the classifications used from previous work. Based on experimental measurements, the flow patterns can be roughly classified into bubbly flow ($0 < S_g < 0.3$), slug flow ($0.3 < S_g < 0.7$), and annular flow region ($0.7 < S_g < 1.0$) for different gas void fractions (Bhagwat, 2011).

2.3. Fixed slip-ratio model

A second commonly used simplification regarding the slippage between different phases is to assume a constant slip ratio:

$$R_{i,j} = \text{Constant} \tag{13}$$

In contrast with the no-slip model, the fixed slip-ratio model requires experimental data to determine the value of $R_{i,j}$ for a given scenario. As illustrated in Fig. 3, each fixed slip-ratio model's fractional flow path stands for a constant $R_{i,j}$ and it varies significantly with the value of $R_{i,j}$. When $R_{i,j}$ is less than 1, the flow path lies below the 45-degree straight line, and the curves' slopes increase with increasing phase volume fraction. Conversely, when the $R_{i,j}$ is greater than 1, the flow paths lie above the 45-degree straight line, and the curves' slopes decrease as the phase volume fraction increases. It is worth noting that the fixed slip-ratio model is not correlation-free due to its reliance on experimental data as inputs.

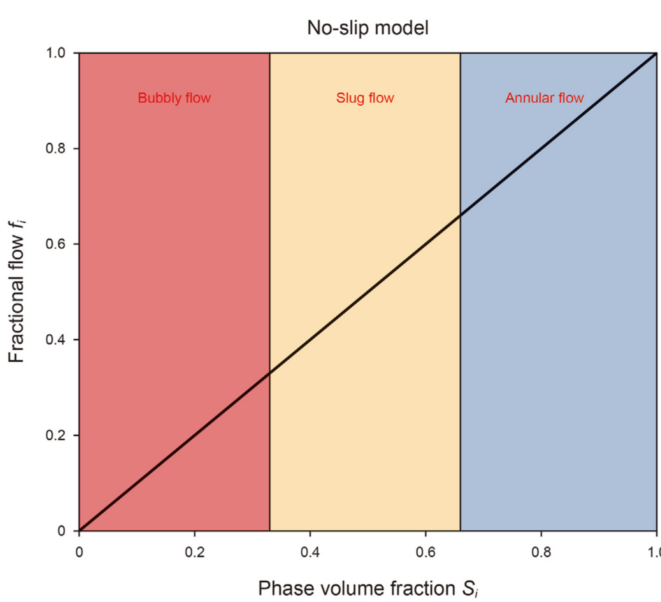

Fig. 2. Fractional flow path for the no-slip model.

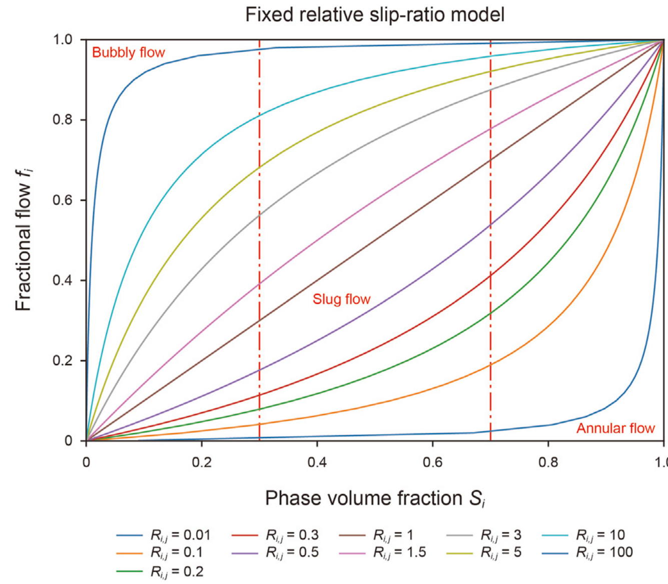

Fig. 3. Fractional flow path for the constant slip-ratio model.

2.4. Power law model

Many data sets that we have analyzed indicate that the slip ratio increases with the fractional flow of phase *i*. An example of such a data set is shown in Fig. 4. The slip ratio at small f_g is about 4 and the slip ratio at large f_g is about 20. As f_g increases, $R_{g,l}$ increases. This suggests that slip ratio ($R_{i,j}$) should be a function of the

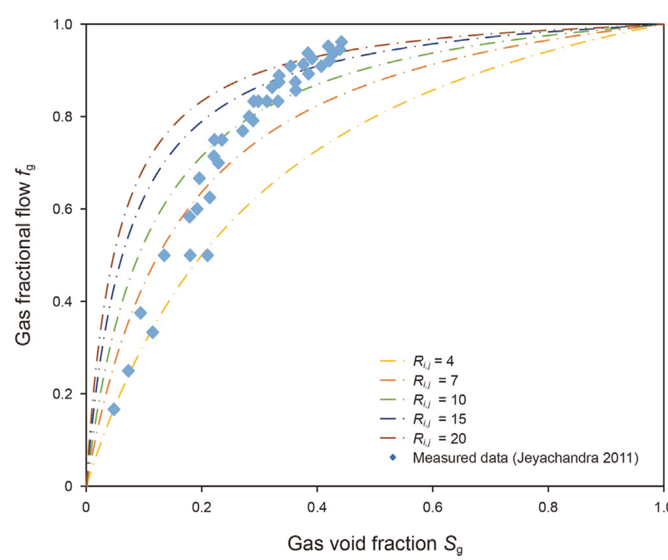

Fig. 4. Slip ratio increases with fractional flow for some experimental datasets.

fractional flow.

We, therefore, propose the following general relationship between $R_{i,j}$ and f_i:

$$R_{i,j} = \left(\frac{1}{1-f_i}\right)^n \tag{14}$$

Substituting Eq. (14) into Eq. (6) and rearranging, an equation correlating the fractional flow of phase i (f_i) and only the volume fraction of phase i (S_i) can be obtained

$$\frac{(1-f_i)^{1-n}}{f_i} = \frac{1-S_i}{S_i} \tag{15}$$

Equivalently, we can rearrange Eq. (15) to express the volume fraction of phase i (S_i) in terms of the fractional flow of phase i (f_i) so that it is in a form consistent with existing void fraction correlations:

$$S_i = \frac{1}{\frac{f_i^{-1}}{(1-f_i)^{n-1}} + 1} \tag{16}$$

According to the relationship between fractional flow and phase volume fraction described in Eq. (15), a series of fraction flow path can be drawn for different n values, as shown below.

Fig. 5 illustrates he non-linear relationship between fractional flow and phase volume fraction. As n increases, the curves shift to the left (the fractional flow increases). Furthermore, when n is equal to zero, the fractional flow path is linear, which is just the no-slip model defined in Section 2.2.

Based on comparisons with 2754 groups of two-phase pipe flow experimental data covering various two-phase fluid systems and operating conditions, we found that Eq. (14) can best fit the data when n equals to 0.5, as seen in Appendix A. Thus, Eqs. (15) and (16) can be expressed as

$$\frac{(1-f_i)^{0.5}}{f_i} = \frac{1-S_i}{S_i} \tag{17}$$

or,

$$S_i = \frac{1}{\frac{f_i^{-1}}{(1-f_i)^{-0.5}} + 1} \tag{18}$$

Despite its simplicity, the power law model can capture the entire range of the multiphase flow conditions in pipes by utilizing the pipe fractional flow theory and the relative slip ratio definition. Fig. 6 illustrates the fractional flow path of the power law model when n is equal to 0.5. It describes the non-linear relationship between fractional flow and phase volume fraction. When the phase volume fraction is less than 0.3, which corresponds to the bubbly flow region, the power law model curve behaves like a straight line, similar to the no-slip model. When the phase volume fraction is in the range of $0.3 < S_g < 0.7$, corresponding to the transition flow region of multiphase flow, the slippage between phases begins to increase. Finally, at phase volume fractions above $S_g > 0.7$, representing the annular or annular mist flow region, the slip reaches its highest values.

2.5. Published empirical correlations in pipe fraction flow framework

Notably, many previously published empirical correlations for gas void fraction or liquid holdup can be reformulated utilizing the pipe fractional flow framework.

Many other past correlations can be expressed in the pipe fractional flow framework in the same way as the Butterworth correlation. Table 1 below takes some well-known correlations and expresses them in terms of the pipe fractional flow and relative slip ratio, many of these correlations are implicit and non-linear and may yield multiple roots for f_g.

Table 1 summarizes some typical empirical phase volume fraction correlations reformulated in the pipe fractional flow framework. Here, we use the Butterworth model as a typical example to demonstrate how it can be re-expressed in the pipe fractional flow framework, and other correlations can be derived in a similar way.

The original form of the Butterworth model is shown as follows:

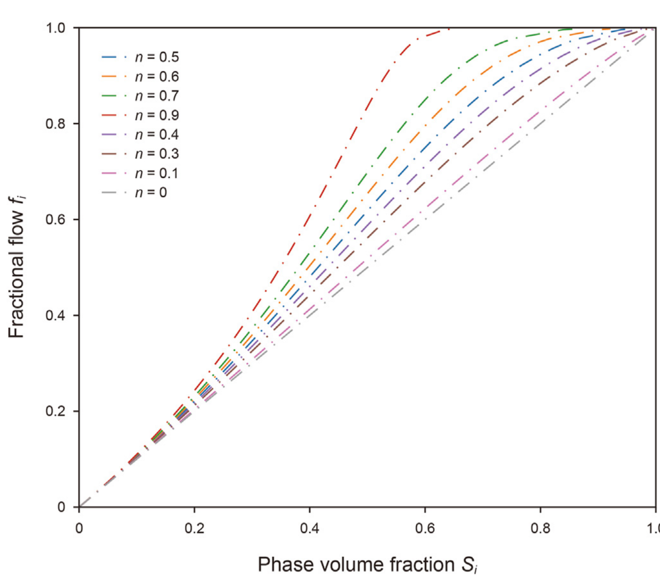

Fig. 5. Fractional flow path upon various n values for power law model.

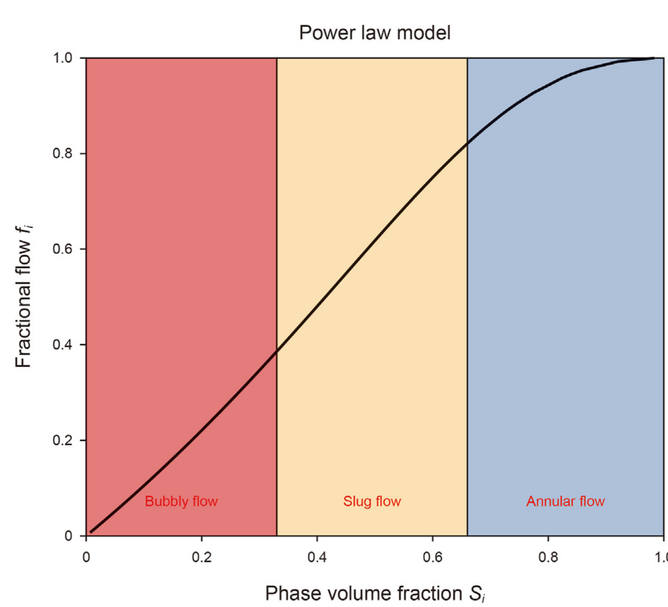

Fig. 6. Fractional flow path for power law model when n is equal to 0.5.

Table 1
Rearranged void fraction correlations by pipe fractional flow theory.

Source	Void fraction correlation	Pipe fractional flow framework
Fauske (1961)	$S_g = \left[1 + \left(\frac{1-x}{x}\right)\frac{\rho_g}{\rho_l}^{0.5}\right]^{-1}$	$\frac{1-f_g}{f_g} = \left(\left(\frac{1-S_g}{S_g}\right)\right)\left(\frac{\rho_g}{\rho_l}\right)^{0.5}$
Baroczy (1966)	$S_g = \left[1 + \left(\frac{1-x}{x}\right)^{0.74}\frac{\rho_g}{\rho_l}^{0.5}\left(\frac{\mu_g}{\mu_l}\right)^{0.13}\right]^{-1}$	$\frac{1-f_g}{f_g} = \left(\left(\frac{1-S_g}{S_g}\right)\left(\frac{\rho_g}{\rho_l}\right)^{0.09}\left(\frac{\mu_g}{\mu_l}\right)^{0.13}\right)^{1.35}$
Thom (1964)	$S_g = \left[1 + \left(\frac{1-x}{x}\right)\frac{\rho_g}{\rho_l}^{0.89}\left(\frac{\mu_g}{\mu_l}\right)^{0.18}\right]^{-1}$	$\frac{1-f_g}{f_g} = \left(\frac{1-S_g}{S_g}\right)\left(\frac{\rho_g}{\rho_l}\right)^{0.11}\left(\frac{\mu_g}{\mu_l}\right)^{0.18}$
Zivi (1964)	$S_g = \left[1 + \left(\frac{1-x}{x}\right)\frac{\rho_g}{\rho_l}^{0.67}\right]^{-1}$	$\frac{1-f_g}{f_g} = \left(\frac{1-S_g}{S_g}\right)\left(\frac{\rho_g}{\rho_l}\right)^{0.33}$
Turner and Wallis (1965)	$S_g = \left[1 + \left(\frac{1-x}{x}\right)^{0.72}\frac{\rho_g}{\rho_l}^{0.4}\left(\frac{\mu_g}{\mu_l}\right)^{0.08}\right]^{-1}$	$\frac{1-f_g}{f_g} = \left(\left(\frac{1-S_g}{S_g}\right)\left(\frac{\rho_g}{\rho_l}\right)^{0.32}\left(\frac{\mu_g}{\mu_l}\right)^{0.08}\right)^{1.39}$
Butterworth (1975)	$S_g = \left[1 + 0.28\left(\frac{1-x}{x}\right)^{0.64}\frac{\rho_g}{\rho_l}^{0.36}\left(\frac{\mu_g}{\mu_l}\right)^{0.07}\right]^{-1}$	$\frac{1-f_g}{f_g} = \left(\left(\frac{1}{0.28}\left(\frac{1-S_g}{S_g}\right)\right)^{1.41}\left(\frac{\rho_g}{\rho_l}\right)^{0.4}\left(\frac{\mu_g}{\mu_l}\right)^{0.1}\right)^{1.11}$

$$S_g = \left[1 + 0.28\left(\frac{1-x}{x}\right)^{0.64}\frac{\rho_g}{\rho_l}^{0.36}\left(\frac{\mu_g}{\mu_l}\right)^{0.07}\right]^{-1} \quad (19)$$

where ρ_g, ρ_l are the density of the gas phase and liquid phase, respectively; μ_g, μ_l are the viscosity of the gas phase and liquid phase, respectively; x is the mass quality, which is defined as the ratio of gas mass flow rate (W_g) to the total mass (W, the sum mass of gas (W_g) and liquid (W_l)) flow rate, as given by

$$x = \frac{W_g}{W_g + W_l} = \frac{W_g}{W} \quad (20)$$

Then $\frac{1-x}{x}$ in the Butterworth model can be derived by employing the definition of the quality (x):

$$\frac{1-x}{x} = \frac{1 - \frac{W_g}{W_g + W_l}}{\frac{W_g}{W_g + W_l}} = \frac{W_l}{W_g} \quad (21)$$

To reformulate the Butterworth model in the pipe fractional flow framework, we need to use fractional flow (f) instead of the quality (x) in the original correlation. Therefore, the term $\frac{1-f_g}{f_g}$ can be similarly obtained by using the definition of fractional flow:

$$\frac{1-f_g}{f_g} = \frac{1 - \frac{Q_g}{Q_g + Q_l}}{\frac{Q_g}{Q_g + Q_l}} = \frac{Q_l}{Q_g} \quad (22)$$

By employing the correlation that the mass flow rate is equal to the product of the phase density and its volumetric flow rate ($W_g = \rho_g Q_g$) in Eq. (21), the final correlation between the fractional flow (f) and the quality (x) can be obtained as

$$\frac{1-x}{x} = \frac{\rho_l Q_l}{\rho_g Q_g} = \left(\frac{\rho_l}{\rho_g}\right)\left(\frac{1-f_g}{f_g}\right) \quad (23)$$

Substituting Eq. (23) into Eq. (19) (original Butterworth model), the new Butterworth model in the pipe fractional flow framework can be expressed as

$$S_g = \left[1 + 0.28\left(\frac{1-f_g}{f_g}\right)^{0.64}\frac{\rho_g}{\rho_l}^{-0.28}\left(\frac{\mu_g}{\mu_l}\right)^{0.07}\right]^{-1} \quad (24)$$

Then, by rearranging the term $\frac{1-f_g}{f_g}$ into the left side and all the remaining terms to the right side of the equation, a final form of the novel Butterworth model in the pipe fractional flow framework is given as

$$\frac{1-f_g}{f_g} = \left(\left(\frac{1}{0.28}\left(\frac{1-S_g}{S_g}\right)\right)^{1.41}\left(\frac{\rho_g}{\rho_l}\right)^{0.4}\left(\frac{\mu_g}{\mu_l}\right)^{0.1}\right)^{1.11} \quad (25)$$

Many other past correlations can be expressed in the pipe

Table 2
Experimental void fraction database.

Data source	Number of data points	Fluid system	Pipe diameter, m	Inclination angle, °	Void fraction, %	Pressure, kPa
Mukherjee (1979)	1171	Air–kerosene	0.0381	−90–90	0.12–0.99	175–659
Beggs (1972)	130	Air–water	0.0254, 0.0381	−10–10	0.116–0.984	241–683
Alkaya (2000)	68	Oil–water	0.0508	−5–5	0–0.95	75–197
Atmaca et al. (2009)	137	Oil–water	0.0508	−5, 0	0–0.97	300
Flores (1997)	135	Oil–water	0.0508	45–90	0.025–0.95	150
Guner (2012)	142	Air–water	0.0762	0–45	0.60–0.99	100–143
Yuan (2011)	57	Air–water	0.1000	0, 5	0.47–0.91	800
Magrini et al. (2012)	140	Air–water	0.0762	0–90	0.975–0.997	0.11–0.15
Minami and Brill (1987)	93	Air–water/kerosene	0.0779	0	0.55–0.99	301–646
Mukhopadhyay (1977)	73	Oil–water	0.0381	−90–90	0.25–0.79	103
Sujumnong (1998)	47	Air–water	0.0117	−90	0.017–0.982	101–233
Vielma et al. (2008)	105	Oil–water	0.0508	0	0.02–0.95	138
Jeyachandra et al. (2012)	350	Air–oil	0.0508	−2, 0, 2	0.01–0.46	140

fractional flow framework in the same way as the Butterworth correlation. Table 1 below takes some well-known correlations and expresses them in terms of the pipe fractional flow and relative slip ratio, many of these correlations are implicit and non-linear and may yield multiple roots for f_g.

3. Void fraction experimental database description

An extensive experimental database consisting of 2754 groups of two-phase pipe flow data from 14 different sources has been compiled, with the majority of the data originating from Tulsa University's TUFFP projects. Table 2 provides detailed information about this database, which covers two-phase flow systems including air–water, air–kerosene, air–oil, and water–oil flows with a wide range of density and viscosity ratios. The flow inclinations encompass upward, downward, upward vertical, downward vertical, and horizontal flows, spanning an inclination angle range of −90° to 90°. The inner diameter of the pipelines varies from 0.0254 to 0.1 m. The combinations of these operating parameters cover the most common two-phase flow patterns

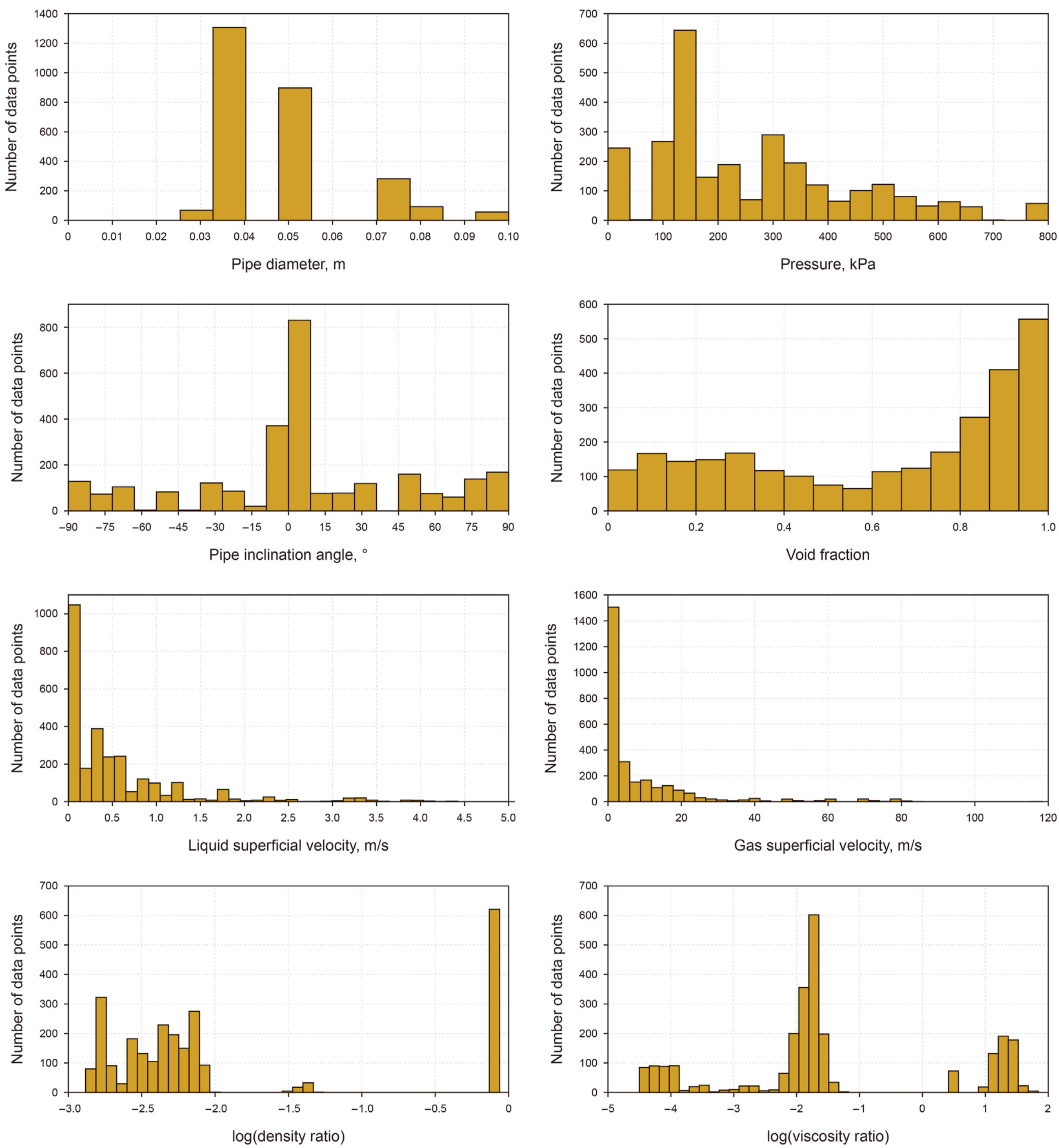

Fig. 7. Selected histograms describing the data distribution in the database.

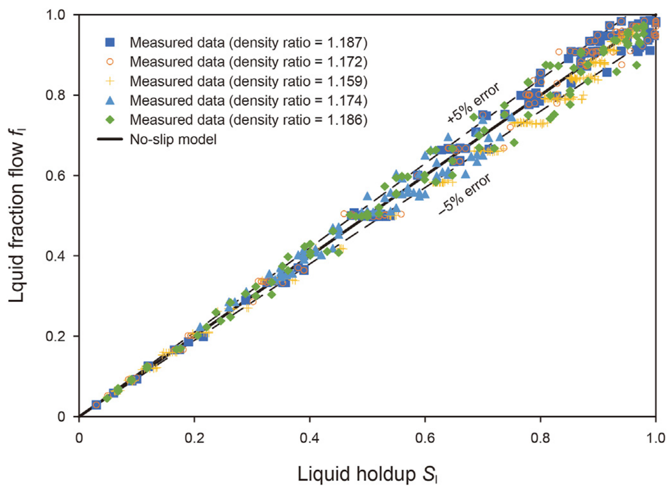

Fig. 8. Verification of no-slip model with experimental data from the database described in Table 2. Only datasets in which the two fluid phases have similar density were selected for this comparison.

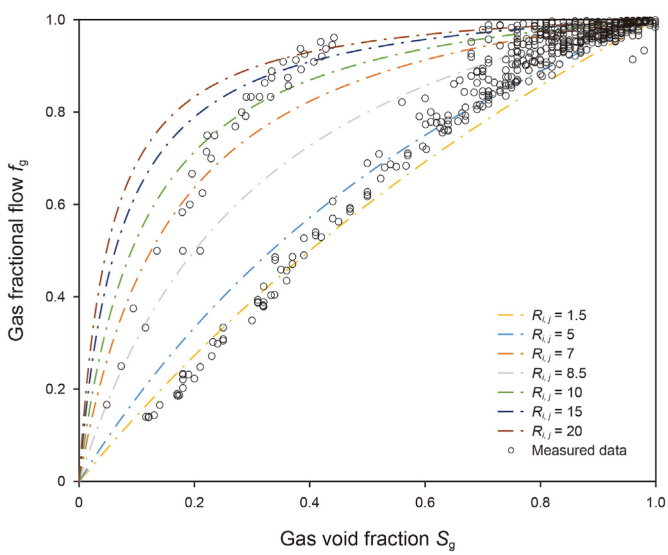

Fig. 9. Verification of fixed slip-ratio model with experimental data described in Table 2.

encountered during oil & gas production including bubble flow, slug flow, and annular flow with concurrent gas–liquid or liquid–liquid flow.

Fig. 7 depicts selected histograms that further describe the distribution of the operating parameters in the experimental database. The operating pressures range from 0 to 800 kPa, with the pressure of most tests falling within the 120–160 kPa range. The gas phase velocity distribution is in the range of 0–120 m/s, with a significant number of data points concentrated in the 0–3 m/s range, whereas the liquid phase velocity distribution ranges from 0 to 5 m/s, with most of the data points concentrated in the 0–0.125 m/s range. Furthermore, a relatively large percentage of gas content (volume void fraction) data falls within the 0.8–1.0 range, with the remaining data almost evenly distributed between 0 and 0.8, encompassing various pipe diameters, inclinations, and fluid properties. This full range of void fraction data (0–1.0) enables the examination of the impacts of different factors on phase volume distributions across different flow patterns. The density and

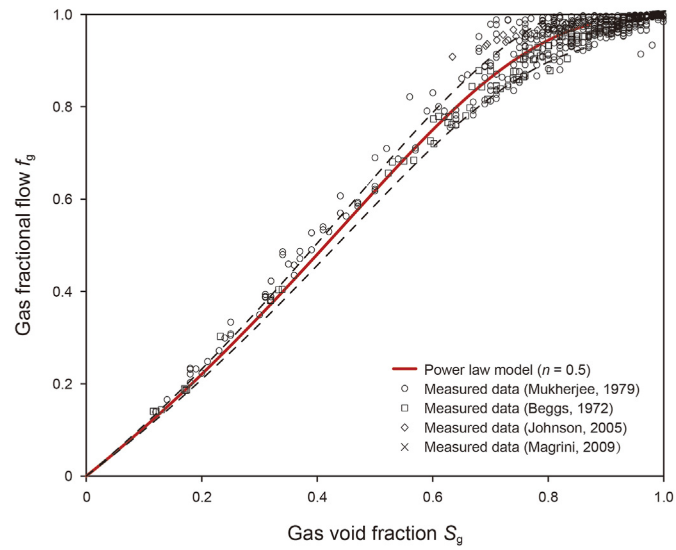

Fig. 10. Verification of power law model with experimental data from the database described in Table 2.

viscosity ratio histograms also display a wide range (−3–0 and −5–2, respectively) on a logarithmic scale, where the density ratio is the ratio of low density to high density. To summarize, this study's database comprises a comprehensive range of two-phase data, reflecting the database's broad coverage.

4. Results and discussion

4.1. The no-slip model

To evaluate the performance of the no-slip model, a comprehensive model verification was conducted using thousands of oil–water datasets encompassing a wide range of conditions from the experimental database, as illustrated in Fig. 8. The results showed that the no-slip model accurately predicted the behavior of the various datasets that use fluids with similar density, demonstrating its ability to provide reliable predictions without any limitations on operating parameters for liquid–liquid systems in which no significant density difference exists between phases.

4.2. The fixed slip-ratio model

Based on the general fractional flow path in Fig. 1, any experimental dataset can be accurately predicted with a pre-known value of $R_{i,j}$. As shown in Fig. 9, all the measured data can be captured by the fractional flow curve with specified slip ratio, namely, the fixed slip-ratio model is capable of predicting accurate gas void fraction with a known slip ratio. Furthermore, the slip ratio increases with increasing gas void fraction, indicating that it is a function of phase volume fraction.

4.3. The power law model

In comparison to existing empirical void fraction correlations, the power law model stands out as an analytical approach that does not rely on any operating parameters such as pipe geometries or fluid properties. Therefore, it is highly desirable to assess the accuracy of the power law model in the prediction of void fraction. To this end, a large set of experimental data from our database, covering different flow patterns, pipe geometries, and flow rates in air–water and air–kerosene systems, was used to verify the

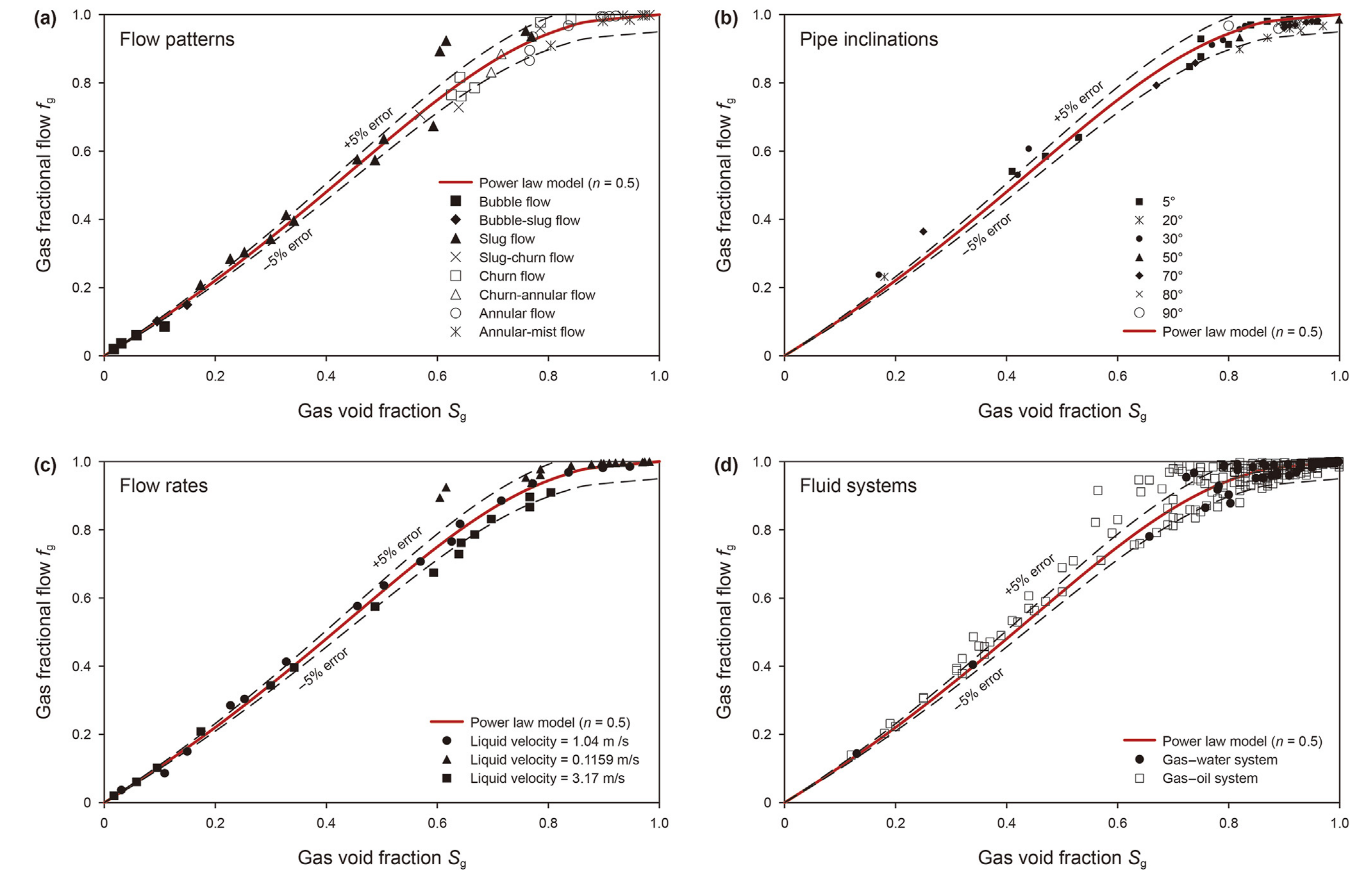

Fig. 11. Accuracy of the power law model in various controllable parameters.

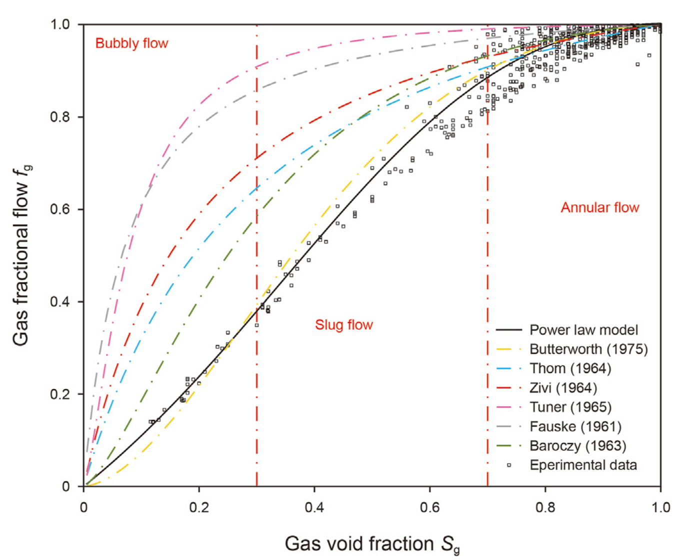

Fig. 12. Comparison of power law model with typical empirical void fraction correlations.

performance of the power law model, as shown in Fig. 10. The comparison results indicate that most of the data fall within the ±5% error bounds of the predictions generated by power law model, and even the data outside these bounds still remain fairly close. These results demonstrate that the power law model can provide precise predictions of the phase volume distribution for any gas–liquid system with a maximum error of ±5%.

To clarify the high accuracy of the power law model in wide-range conditions, the comprehensive validation was conducted in relation to individual parameters, including flow patterns, pipe inclination, flow rates, and fluid systems as illustrated in Fig. 11. In each subplot in Fig. 11, the black curve depicts the fractional flow path generated from the power law model, along with various data points representing the selected experimental data from our database covering full range of flow patterns, the pipe inclination angles ranging from 5° to 90°, liquid flow rates of 0.1159, 1.04, and 3.17 m/s and two types of fluid systems referring to the gas–water and gas–oil systems. The results demonstrate that almost all the measured data lies within the range of ±5% error or in close proximity to the ±5% error lines, indicating that the power law model can provide reliable prediction of the phase volume fraction under various controllable parameters. This surpasses the limitations of typical empirical void fraction correlations.

Furthermore, the performance of power law model is compared with those of other typical empirical void fraction correlations to demonstrate its the advantage and accuracy, and the comparisons are shown in Fig. 12. The datasets used for this comparison contain all flow patterns, various geometries, and fluid properties. The results in Fig. 12 show that the power law model has the highest accuracy in all conditions for a gas–liquid flow system. The second accurate method is Butterworth's (1975) model, which can capture most of the data for a gas–liquid system. Other models only perform well in the annular flow region, which corresponding to a void fraction of 0.7–1.0.

Table 3
Recommended pipe fractional flow model for various two-phase flow in pipes.

Fluid system	Pipe inclination	Pipe fractional flow models
Gas–liquid	Horizontal (0°)	Power law model ($n = 0.5$) (best)
	Upward vertical (90°)	Fixed slip-ratio model
	Upward inclined (0°–90°)	
	Downward vertical (−90°)	Fixed slip-ratio model (best)
	Downward inclined (0°–90°)	
Liquid–liquid	All	No-slip model (best)
		Fixed slip-ratio model

4.4. Recommendations for applicable pipe fractional flow model

Based on the results shown above, the following recommendations are provided for the conditions under which the different models can be used.

(a) The no-slip model is most accurate for liquid–liquid systems or other two-phase flow systems in which the two phases have similar densities.
(b) The fixed slip-ratio model is applicable in all types of two-phase flow systems with known slip ratios ($R_{i,j}$)
(c) The power law model performs best in gas–liquid systems with upward-vertical, upward-inclined and horizontal inclinations.

These findings are summarized in Table 3 with the best method for each scenario identified.

5. Conclusions

Reliable calculations of gas void fraction (or liquid holdup) play a central role in two-phase pipe flow models. Following the pioneer work by Nagoo and Sharma (Nagoo, 2014, 2019; Nagoo and Sharma, 2017), we present a unified modeling framework capable of predicting the phase volume fraction over a broad range of conditions for two-phase pipe flow. The model was reformulated from the fractional flow theory for multiphase porous media flows and adapted to multiphase pipe flow. The fractional flow path was correlated with the phase distributions and relative slippage ratios. Different treatments of the slippage ratios lead to three different simplified models, the no-slip model, the fixed slip-ratio model, and the power law model. The fixed slip-ratio model is applicable in all types of two-phase flow systems with a known slip ratio. The no-slip model is most accurate for liquid–liquid systems or other two-phase flow systems in which the two phases have similar densities, whereas the power law model performs best in gas–liquid systems with upward-vertical, upward-inclined and horizontal inclinations. Compared to existing methods and correlations, this new framework provides a simple yet sufficient way to estimate the phase volume fraction in two-phase pipe flow without referring to the influential operating variables such as pipe geometries, fluid properties, and flow patterns. The models also provide a continuous variation of fluid flow velocities over the entire range of fluid saturations (as opposed to breaks and discontinuities in the flow velocities that are imposed by the introduction of flow patterns). Notably, existing correlations for estimating phase volume fraction can be transformed and adapted under the fractional flow modeling framework. The developed model demonstrates high accuracy with 5% margin of error and broad applicability when verified against an experimental database comprised of 2754 data groups from 14 literature sources, covers a wide range of gas velocities (0–120 m/s) and liquid velocities (0–3 m/s), pipe diameters (25.4–100 mm), pressures (0–800 kPa), pipe inclinations (−90°–90°), logarithmic of density ratios (−3–0), logarithmic of viscosity ratios (−5–2), and flow patterns including bubble, slug, and annular flow.

CRediT authorship contribution statement

Fuqiao Bai: Writing – original draft, Visualization, Validation, Software, Methodology, Investigation, Formal analysis, Conceptualization. **Yingda Lu:** Writing – review & editing, Validation, Supervision, Resources, Project administration, Methodology, Funding acquisition. **Mukul M. Sharma:** Writing – review & editing, Validation, Supervision, Resources, Project administration, Methodology, Funding acquisition.

Declaration of competing interest

The authors declare that they have no known competing financial interests or personal relationships that could have appeared to influence the work reported in this paper.

Acknowledgments

We gratefully acknowledge the financial support from the Energize Program between the University of Texas at Austin and Southwest Research Institute. We would also like to express our gratitude to the Hydraulic Fracturing and Sand Control Industrial Affiliates Program at the University of Texas at Austin for financially supporting this research.

Appendix A. Parameter *n* validation for relationship between fractional flow and slip ratio

The appendix provides regression result for the relationship between fractional flow and slip ratio with total 2753 data points in the database. The regression shows the best fit function comes from n at a value of 0.5.

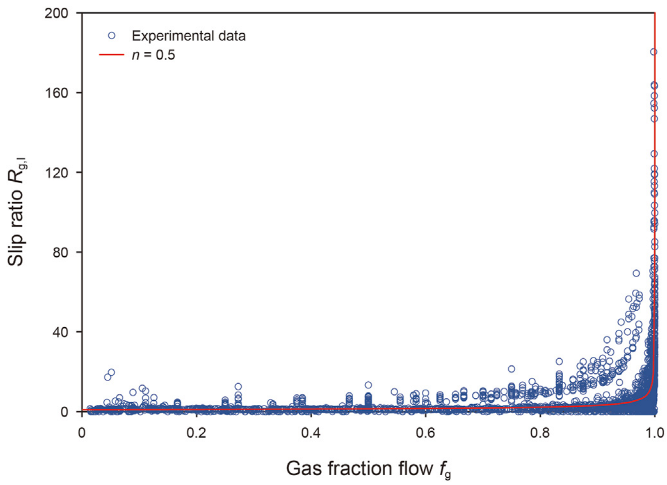

Fig. A1. Static regression with experimental data for the parameter n in function between fractional flow and slip ratio.

References

Alkaya, B., 2000. Oil-water Flow Patterns and Pressure Gradients in Slightly Inclined Pipes. Doctoral Dissertation. University of Tulsa.

Abdul-Majeed, G., 1996. Liquid holdup in horizontal two-phase gas–liquid flow. J. Petrol. Sci. Eng. (15 (2–4)), 271–280. https://doi.org/10.1016/0920-4105(95)00069-0.

Armand, A.A., 1946. The resistance during the movement of a two-phase system in horizontal pipes. Izv. Vses. Teplotekh. Inst. 15, 16–23.

Atmaca, S., Sarica, C., Zhang, H.-Q., Al-Sarkhi, A., 2009. Characterization of oil/water flows in inclined pipes. SPE Proj. Facil. Constr. 4 (2), 41–46. https://doi.org/10.2118/115485-PA.

Bai, F., Lou, W., Lu, Y., 2023. A robust drift-flux model for two-phase CO_2 pipe flow. Gas Sci. Eng. 119, 205140. https://doi.org/10.1016/j.jgsce.2023.205140.

Baroczy, C., 1966. Systematic Correlation for Two-phase Pressure Drop. Atomics International, Canoga Park, Calif.

Beggs, H.D., 1972. An Experimental Study of Two-phase Flow in Inclined Pipes. The University of Tulsa.

Bhagwat, S.M., 2011. Study of Flow Patterns and Void Fraction in Vertical Downward Two Phase Flow. Oklahoma State University.

Bhagwat, S.M., Ghajar, A.J., 2014. A flow pattern independent drift flux model based void fraction correlation for a wide range of gas–liquid two phase flow. Int. J. Multiphas. Flow 59, 186–205. https://doi.org/10.1016/j.ijmultiphaseflow.2013.11.001.

Butterworth, D., 1975. A comparison of some void-fraction relationships for co-current gas-liquid flow. International Journal of Multiphase Flow 1 (6), 845–850. https://doi.org/10.1016/0301-9322(75)90038-5.

Choi, J., Pereyra, E., Sarica, C., Park, C., Kang, J.M., 2012. An efficient drift-flux closure relationship to estimate liquid holdups of gas-liquid two-phase flow in pipes. Energies 5 (12), 5294–5306. https://doi.org/10.3390/en5125294.

Cioncolini, A., Thome, J.R., 2012. Void fraction prediction in annular two-phase flow. Int. J. Multiphas. Flow 43, 72–84. https://doi.org/10.1016/j.ijmultiphaseflow.2012.03.003.

Czop, V., Barbier, D., Dong, S., 1994. Pressure drop, void fraction and shear stress measurements in an adiabatic two-phase flow in a coiled tube. Nuclear Engineering and Design 149 (1–3), 323–333. https://doi.org/10.1016/0029-5493(94)90298-4.

Fauske, H., 1961. Critical two-phase, steam–water flows. Proceedings of the 1961 Heat Transfer and Fluid Mechanics Institute. Stanford University Press, Stanford, CA, pp. 79–89.

Flores, J.G., 1997. Oil-water Flow in Vertical and Deviated Wells. The University of Tulsa.

Gao, Q., Wang, Z., Zeng, Q., 2021. A unified model of oil/water two-phase flow through the complex pipeline. Geofluids 1–9. https://doi.org/10.1155/2021/3756577.

Guner, M., 2012. Liquid loading of gas wells with deviations from 0 to 45. University of Tulsa.

Hughmark, G., 1962. Holdup in gas-liquid flow. Chem. Eng. Prog. 58 (4), 62–65.

Jeyachandra, B.C., Sarica, C., Zhang, H.-Q., Pereyra, E., 2012. Inclination effects on flow characteristics of high viscosity oil/gas two-phase flow. In: SPE Annual Technical Conference and Exhibition. https://doi.org/10.2118/159217-MS.

Jia, H., Zhu, J., Cao, G., Lu, Y., Lu, B., Zhu, H., 2022. A model ranking approach for liquid loading onset predictions. SPE Prod. Oper. 37 (3), 370–382. https://doi.org/10.2118/209578-PA.

Jowitt, D., Cooper, C., Pearson, K., 1984. The THETIS 80% blocked cluster experiment. Part 5. No. AEEW-R–1767.UKAEA Atomic Energy Establish.

Li, N.-L., Chen, B., 2023. Evaluation of frictional pressure drop correlations for air-water and air-oil two-phase flow in pipeline-riser system. Petrol. Sci. 21 (2), 1305–1319. https://doi.org/10.1016/j.petsci.2023.09.020.

Lockhart, R., Martinelli, R., 1949. Proposed correlation of data lor isothermal two-phase, two-component flow in pipes. Chem. Eng. Progress. 45 (1), 39–48.

Lou, W.-Q., Sun, D.-L., Sun, X.-H., Li, P.-F., Liu, Y.-X., Guan, L.-C., et al., 2023. High-precision nonisothermal transient wellbore drift flow model suitable for the full flow pattern domain and full dip range. Petrol. Sci. 20 (1), 424–446. https://doi.org/10.1016/j.petsci.2022.11.011.

Magrini, K.L., Sarica, C., Al-Sarkhi, A., Zhang, H.-Q.-Q., 2012. Liquid entrainment in annular gas/liquid flow in inclined pipes. SPE J. 17 (2), 617–630. https://doi.org/10.2118/134765-PA.

Márquez-Torres, L., Ochoa-Pineda, J., Pico, P., Valdés, J.P., Becerra, D., Pinilla, A., et al., 2020. Comparison of 63 different void fraction correlations for different flow patterns, pipe inclinations, and liquid viscosities. SN Appl. Sci. 2, 1–24. https://doi.org/10.1007/s42452-020-03464-w.

Massena, W., 1960. Steam-water Pressure Drop and Critical Discharge Flow-A Digital Computer Program. General Electric Co. Hanford Atomic Products Operation, Richland, Wash.

Minami, K., Brill, J., 1987. Liquid holdup in wet-gas pipelines. SPE Prod. Eng. 2 (1), 36–44. https://doi.org/10.2118/14535-PA.

Mukherjee, H., 1979. An Experimental Study of Inclined Two-phase Flow. The University of Tulsa.

Mukhopadhyay, H., 1977. An Experimental Study of Two-phase Oil-Water Flow in Inclined Pipes. University of Tulsa. Fluid Flow Projects.

Nagoo, A.S., 2014. Pipe Fractional Flow Theory: Principles and Applications. Doctoral Dissertation. The University of Texas at Austin.

Nagoo, A.S., 2019. First wholly-analytical gas volume fraction model for virtual multiphase flow metering petroleum industry applications. Int. J. EQ. 4 (2), 244–254.

Nagoo, A.S., Sharma, M.M., 2017. Finer theoretical aspects of the drift flux family of equations for simulating averaged volume fraction in multiphase flows. Int. J. CMEM. 6 (2), 240–250.

Nicklin, D., 1962. Two-phase flow in vertical tubes. Trans. Inst. Chem. Eng. 40 (1), 61–68.

Spedding, P., Chen, J., 1984. Holdup in two phase flow. Int. J. Multiphas. Flow 10 (3), 307–339. https://doi.org/10.1016/0301-9322(84)90024-7.

Sujumnong, M., 1998. Heat transfer, pressure drop and void fraction in two-phase, two-component flow in a vertical tube. Doctoral Dissertation. The University of Manitoba.

Sun, J., Guo, L., Fu, J., Jing, J., Yin, X., Lu, Y., et al., 2022. A new model for viscous oil-water eccentric core annular flow in horizontal pipes. Int. J. Multiphas. Flow 147, 103892. https://doi.org/10.1016/j.ijmultiphaseflow.2021.103892.

Sun, J., Guo, L., Jing, J., Duan, L., Lu, Y., Ullmann, A., et al., 2021a. A comparison of numerical simulations with experimental and theoretical investigations of highly-viscous oil-aqueous foam horizontal flow. J. Petrol. Sci. Eng. 201, 108507. https://doi.org/10.1016/j.petrol.2021.108507.

Sun, J., Guo, L., Jing, J., Tang, C., Lu, Y., Fu, J., et al., 2021b. Investigation on laminar pipe flow of a non-Newtonian Carreau-Extended fluid. J. Petrol. Sci. Eng. 205, 108915. https://doi.org/10.1016/j.petrol.2021.108915.

Sunday, N., Settar, A., Chetehouna, K., Gascoin, N., 2023. Numerical modeling and parametric sensitivity analysis of heat transfer and two-phase oil and water flow characteristics in horizontal and inclined flowlines using OpenFOAM. Petrol. Sci. 20 (2), 1183–1199. https://doi.org/10.1016/j.petsci.2022.10.008.

Teixeira, R.G., Secchi, A.R.Biscaia, E, C., 2015. Differential-algebraic approach to solve steady-state two-phase flow drift-flux model with phase change. Computer Aided Chem. Eng. 317–322. https://doi.org/10.1016/B978-0-444-63578-5.50048-7.

Thom, J., 1964. Prediction of pressure drop during forced circulation boiling of water. Int. J. Heat Mass Tran. 7 (7), 709–724. https://doi.org/10.1016/0017-9310(64)90002-X.

Turner, J., Wallis, G., 1965. The separate-cylinders model of two-phase flow. Paper No. NYO-3114-6. Thayer's School Engineering, Dartmouth College, Hanover, NH, USA.

Vielma, M., Atmaca, S., Sarica, C., Zhang, H., 2008. Characterization of oil/water flows in horizontal pipes. SPE Proj. Facil. Constr. 3 (4), 1–21. https://doi.org/10.2118/109591-PA.

Vijayan, P., Patil, A., Pilkhwal, D., Saha, D., Venkat Raj, V., 2000. An assessment of pressure drop and void fraction correlations with data from two-phase natural circulation loops. Heat Mass Tran. 36 (6), 541–548. https://doi.org/10.1007/s002310000108.

Woldesemayat, M.A., 2006. Comparison of Void Fraction Correlations for Two-phase Flow in Horizontal and Upward Inclined Flows. Oklahoma State University.

Woldesemayat, M.A., Ghajar, A.J., 2007. Comparison of void fraction correlations for different flow patterns in horizontal and upward inclined pipes. Int. J. Multiphas. Flow 33 (4), 347–370. https://doi.org/10.1016/j.ijmultiphaseflow.2006.09.004.

Yu, H.-Y., Xu, Q., Cao, Y.-Q., Huang, B., Wang, H.-X., Guo, L.-J., 2023. Characterizations of gas-liquid interface distribution and slug evolution in a vertical pipe. Petrol. Sci. 20 (5), 3157–3171. https://doi.org/10.1016/j.petsci.2023.03.009.

Yuan, G., 2011. Liquid Loading of Gas Wells. University of Tulsa.

Zivi, S., 1964. Estimation of steady-state steam void-fraction by means of the principle of minimum entropy production. J. Heat Tran. 86 (2), 247–251. https://doi.org/10.1115/1.3687113.

Zuber, N., Findlay, J.A., 1965. Average volumetric concentration in two-phase flow systems. J. Heat Tran. 87 (4), 453–468. https://doi.org/10.1115/1.3689137.